SHEAR BEHAVIOR OF POLYPROPYLENE FIBER REINFORCED ECC BEAMS WITH VARYING SHEAR REINFORCEMENT RATIOS

Rui ZHANG[1], Koji MATSUMOTO[2], Takayoshi HIRATA[3], Yoshikazu ISHIZEKI[4] and Junichiro NIWA[5]

[1]Member of JSCE, PhD Candidate, Dept. of Civil Eng., Tokyo Institute of Technology
(2-12-1-M1-17, Ookayama, Tokyo 152-8552, Japan)
E-mail: zhang.r.ab@m.titech.ac.jp
[2]Member of JSCE, Assistant Professor, Dept. of Civil Eng., Tokyo Institute of Technology
(2-12-1-M1-17, Ookayama, Tokyo 152-8552, Japan)
E-mail: matsumoto.k.ar@m.titech.ac.jp
[3]Member of JSCE, Research Engineerer, Dept. of Construction and Materials., Technical Research Institute of Obayashi Corporation
(640, Shimokiyoto 4-chome, Kiyose-shi, Tokyo 204-8558, Japan)
E-mail: hirata.takayoshi@obayashi.co.jp
[4]Member of JSCE, Research Engineerer, Dept. of Construction and Materials., Technical Research Institute of Obayashi Corporation
(640, Shimokiyoto 4-chome, Kiyose-shi, Tokyo 204-8558, Japan)
E-mail: ishizeki.yoshikazu@obayashi.co.jp
[5]Fellow of JSCE, Professor, Dept. of Civil Eng., Tokyo Institute of Technology
(2-12-1-M1-17, Ookayama, Tokyo 152-8552, Japan)
E-mail: jniwa@cv.titech.ac.jp

The effects of reducing shear reinforcement ratio in polypropylene fiber reinforced engineered cementitious composites (PP-ECC) beams were investigated in this study. A normal RC control beam was prepared with providing an amount of shear reinforcements. Furthermore, five specimens using PP-ECC were fabricated with monotonic reducing shear reinforcement ratio from the level of RC control beam to zero. And there is also another RC beam without shear reinforcement in shear span was prepared for comparison. Based on the experimental results obtained, it was found that the shear carried by PP-ECC in the beam decreased as the increase in shear reinforcement ratio. This is because of the sliding along the critical crack surface which damaged the bridging effect of fibers. If the reduction of shear carried by fibers is caused due to increasing shear reinforcement, it may result in overestimation of shear strength for PP-ECC structural members.

Key Words : *shear behavior, PP-ECC, shear reinforcement ratio, shear tension failure*

1. INTRODUCTION

Polypropylene Fiber Reinforced Engineered Cementitious Composites (PP-ECC, referred herein after), as one kind of ECCs, exhibits multiple fine cracking, pseudo strain hardening behavior and high ductility under uniaxial tensile loading. It has higher tensile strength compared to normal concrete and has capability of reaching ultimate tensile strain between 1 and 5% under monotonic loading. Its pseudo strain-hardening behavior results from its unique multiple fine cracking mechanism, in which closely spaced fine cracks form because of the bridging action of fibers [1), 2)]. Different from the normal concrete in mixture, ECC generally uses fine aggregates and relatively low volume fractions of short and random fibers (approximately 2 to 3%). Since the absence of coarse aggregate, the elastic modulus of ECC is comparatively lower than that of normal concrete while its compressive strength is equivalent to that of normal concrete.

So far, various types of fiber have been utilized to produce ECCs, including steel, carbon and polymer fibers[1)]. Most structural and retrofit application of ECC reported in the literature use ultra-high molecular weight polyethylene (PE) and polyvinyl alcohol

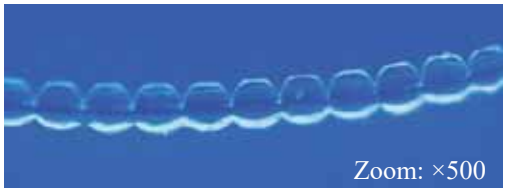

Fig. 1 Cross section of PP fiber

Table 1 Properties of polypropylene fiber

Fiber type	Length (mm)	Diameter (μm)	Young's modulus (MPa)	Tensile strength (MPa)
Polypropylene (PP)	12	36	5000	482

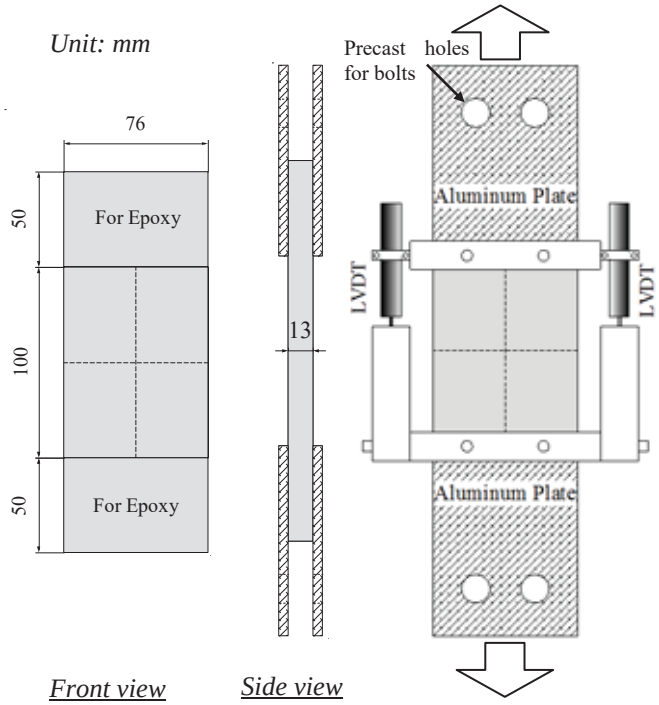

(a) Dimensions of specimen (b) Setup of tests

Fig. 2 Uniaxial tensile tests of PP-ECC

Table 2 Mix proportion of ECC

W/C	Unit (kg/m^3)			
(%)	Water	Cement	PP Fiber	AE
27	371	1400	27	7

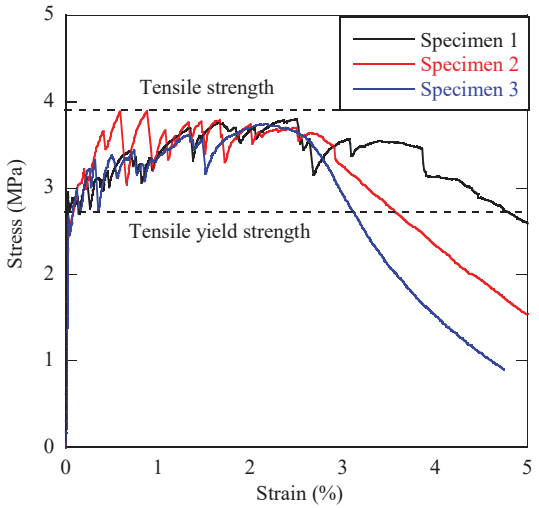

Fig. 3 Results of uniaxial tensile tests

(PVA) fibers. Compared with widely used PVA fibers, polypropylene (PP) fiber is softer, lower cost and easier dispersing which results in better workability. In addition, because of hydrophobic and non-polar nature of PP fiber, PP-ECC has better durability in alkaline environment[3]. In this research, a cementitious composite combined with fabricated polypropylene fibers with improved bond properties (**Fig. 1**) that exhibits the pseudo strain hardening and multiple fine cracking of ECCs[4] was used. The properties of PP fiber are shown in **Table 1**.

Although the steel reinforced ECC (R/ECC) structural members such as column and beam-column joints with reduction of shear reinforcements[5), 11)] have been confirmed in previous studies, the shear behavior of ECC beams with reduction of shear reinforcements has not been completely clarified yet. Therefore, Shimuzu et al.[6)] have done several experimental programs on evaluating the shear behavior of PVA-ECC beams by conducting Ohno-type shear tests and uniaxial tensile tests. The shear strength of tested beams was predicted by employing truss-and-arch model with reduced tensile strength which was obtained from the uniaxial tensile tests. However, Kabele et al.[10)] revealed that only a fraction of ECC's tensile strength and strain capacity might be utilized in shear elements due to possible damage of bridging fibers on sliding crack surfaces. However, there is no study on the reduction factor of tensile strength of ECC due to the sliding on the crack surfaces. Therefore, investigating reduction factor for PP-ECC tensile strength is the key to evaluate the shear strength of PP-ECC beams precisely.

In this research, totalling five PP-ECC and two normal RC beams with various shear reinforcement ratios were tested to clarify shear behavior. The tensile properties of ECC were obtained from uniaxial tensile tests. The reduction factor was evaluated in this study.

2. UNIAXIAL TENSILE TESTS OF PP-ECC

Tensile behavior, as one of the most important characteristics of ECC, was investigated by uniaxial tensile tests. PP-ECC material used in this research is a class of short-fiber, randomly distributed cementitious composites with 3% fiber volume fraction. The polypropylene fiber has a diameter of 36 μm and a

length of 12 mm. The modulus of elasticity and tensile strength of this fiber are 5 GPa and 480 MPa, respectively. This fibrillated polypropylene fiber with rugged surface as shown in **Fig. 1** results in improvement of bond properties and exhibits the pseudo strain hardening and multiple fine cracking of ECC under tensile stress[3]. The mixture proportion of PP-ECC used in this study is shown in **Table 2**.

(1) Specimen layout and test method

Tensile properties of PP-ECC were also inspected by employing uniaxial tensile method. The specimens for uniaxial tensile tests were plates with cross sectional size of 76×13 mm, as shown in **Fig. 2(a)**. The epoxy was used to glue both sides of plate specimens with aluminium plates so that they could be hinged with loading steel by two bolts at each side. Before loading tests, a specimen together with fixed loading steel were set into testing facility.

Two linear variable differential transformers (LVDTs) set parallel to the loading direction at both sides, as shown in **Fig. 2(b)**, were used to measure the axial deformation. 0.1 mm/min was selected as the head speed of loading facility.

(2) Test results

Tensile stress versus strain curves of three specimens are shown in **Fig. 3**. The test result clearly shows typical pseudo strain hardening behavior of ECCs. From the beginning of tests, the stress continued to increase until occurrence of the first crack. The stress then suddenly decreased, whereas it continued to increase after this sudden decrease resulting from occurrence of the first crack. As the loading continued, the increase and sudden decrease of stress continued to take place. Meanwhile, more and more fine cracks were observed on the surface of the specimen. At the strain around 3%, a localized crack gradually formed and the stress began to decrease slowly. The tesnsile yield strength is determined to the lower value immediately after first cracking based on the stress-strain relationship, and the tensile strength is defined as the maximum stress in the tensile stress-strain curve obtained from uniaxial tensile tests. In this study, the yield and tensile strength were greater than 2 and 3 MPa, respestively.

3. BEAM TESTS PROGRAM

(1) Steel reinforcements

A regular deformed steel reinforcing bar with nominal diameter of 25.4 mm and yield strength of 400 MPa was used for longitudinal reinforcement in tension in all beam specimens. The shear reinforcement was adopted deformed bar with nominal

Table 3 Properties of steel reinforcements

Steel bars	Nominal diameter (mm)	f_y (MPa)	f_u (MPa)	ε_u	ε_y
Rebar in tension	25.4	400	577	0.22	0.002000
Shear reinforcements	6.35	323	499	0.17	0.001615
Rebar in compression	6	277	434	0.33	0.001385

f_y is yield strength; f_u is ultimate strength; ε_u is ultimate strain; ε_y is yield strain.

Table 4 Mix proportion of concrete

G_{max}	W/C	Unit (kg/m^3)				
(mm)	(%)	Water	Cement	Fine aggregate	Coarse aggregate	Superplasticizer
20	60	176.6	294.3	829.9	970.3	2.943

G_{max} is the maximum size of coarse aggregate.

Table 5 Summary of beam specimens

Specimen designation	Length L (mm)	Shear reinforcements		Longitudinal bar		Matrix type
		r_w (%)	s (mm)	A_s (mm^2)	p_w (%)	
RC-Ref	2100	0.42	100	1013.4	2.7	Concrete
RC-00		0.00	–			
RE-42		0.42	100			ECC
RE-30		0.30	140			
RE-24		0.24	175			
RE-12		0.12	350			
RE-00		0.00	–			

r_w is shear reinforcement ratio. s is the spacing of shear reinforcements. A_s is the total cross sectional area of longitudinal reinforcements. p_w is the longitudinal reinforcement ratio.

diameter of 6.35 mm and yield strength of 323 MPa. The round steel bar with diameter of 6 mm and yield strength of 277 MPa was used for longitudinal reinforcement in compression. The type and properties of all steel bars used in these seven beam specimens are summarized in **Table 3**.

(2) PP-ECC and concrete

PP-ECC material used in this research is as described in **Chapter 2**. The mixture proportion of PP-ECC used in this study is shown in **Table 2**.

For normal concrete beams, concrete with a design compressive strength of 27 MPa was used. Mixture components include 20 mm maximum size coarse aggregate, fine aggregate and high-early strength cement. **Table 4** gives the mix proportion of normal concrete.

(3) Layout of test specimens

Two different types of matrixes (concrete and PP-ECC), totalling seven beams, including one control beam (RC-Ref), one RC beam without shear reinforcement within the shear span (RC-00) and five PP-ECC beams with varying shear reinforcement ratio from the level of control beam to zero, as summarized in **Table 5**, were tested by four-point loading method as shown in **Fig. 4**. The designations of these seven specimens were selected according to their matrix type and shear reinforcement ratio. 'RC' and 'RE' indicate that the matrix type of the specimen was 'Reinforced Concrete' and 'Reinforced ECC', respectively. Except the case of control beam (RC-Ref), the latter digit in specimen designations indicates the shear reinforcement ratio, e.g. RE-24 implies the specimen with shear reinforcement ratio of 0.24% using steel reinforced ECC.

All beam specimens had the same cross-sectional dimension (150×300 mm), longitudinal reinforce-

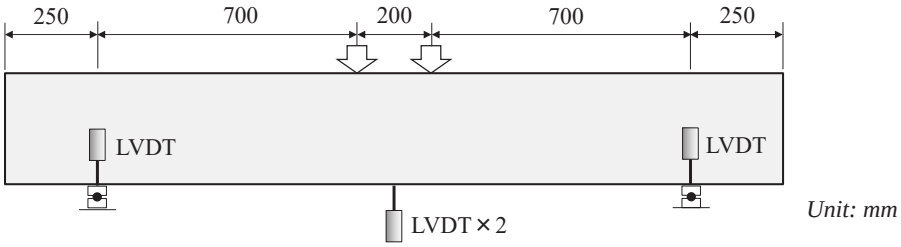

Fig. 4 Experimental setup

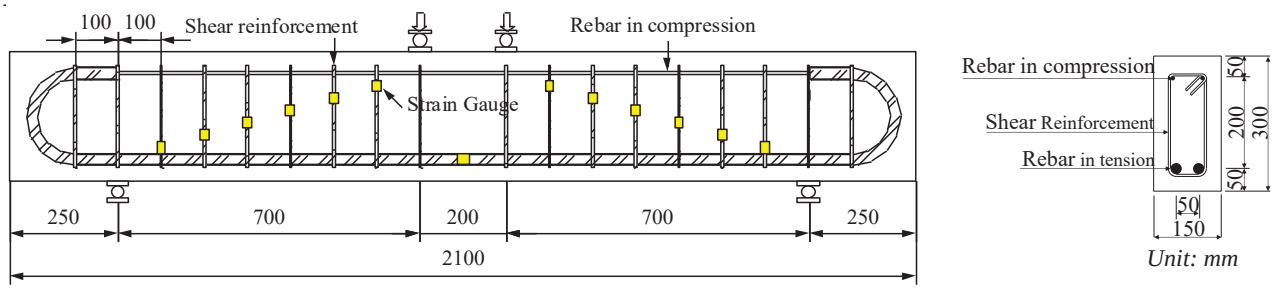

Fig. 5 Dimensions and reinforcement details of RC-Ref and RE-42

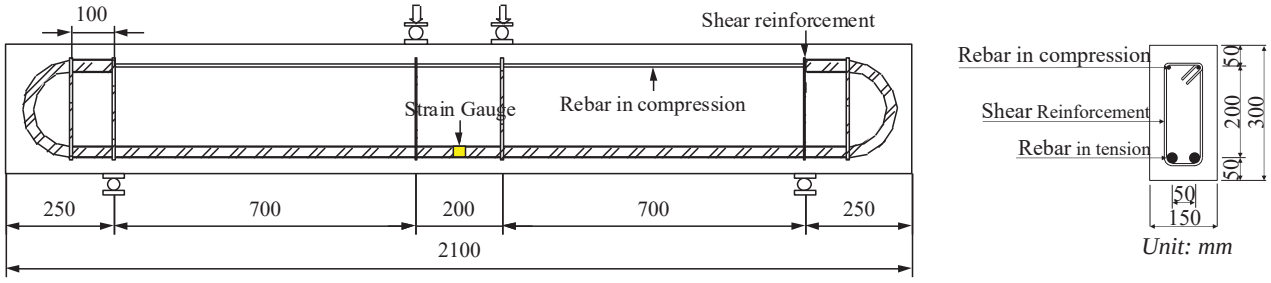

Fig. 6 Dimensions and reinforcement details of RC-00 and RE-00

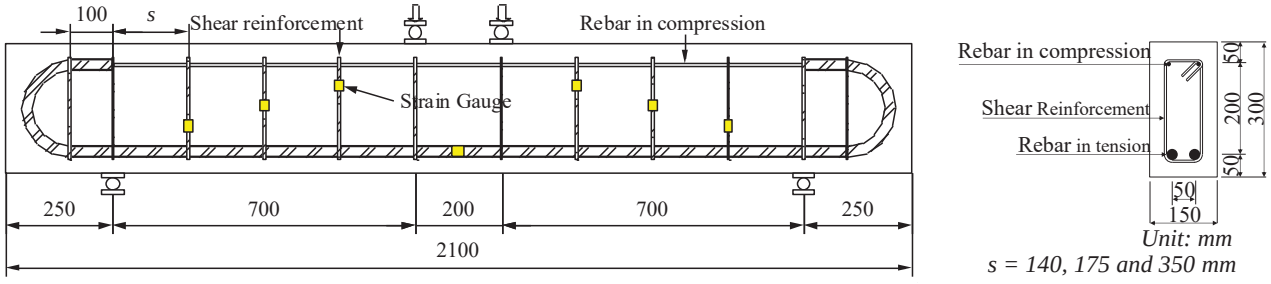

Fig. 7 Dimensions and reinforcement details of RE-30, 24 and 12

ments and shear span-effective depth ratio. The normal concrete beam, RC-Ref was designed following JSCE code, providing exactly equivalent amount of shear reinforcements in both shear span symmetrically (six shear reinforcements in one shear span) which satisfied an under-reinforced condition. The beam specimen corresponding RC-Ref using PP-ECC, namely RE-42, having identical shear reinforcement ratio to normal concrete control beam RC-Ref, was also prepared for comparisons. The dimension and reinforcement details of these two beam specimens are as shown in **Fig. 5**. To evaluate the shear behavior without shear reinforcements, another normal concrete beam specimen RC-00 without shear reinforcements was designed to compare the shear capacity with the specimen RE-00 with identical reinforcement but using matrix of PP-ECC. The dimension and reinforcement arrangement are shown in **Fig. 6**. For the rest three PP-ECC beam specimens, the shear reinforcement ratios varied from 0.30 to 0.12%. All shear reinforcements were uniformly arranged within the shear span as shown in **Fig. 7**.

(4) Test setup and procedure

The arrangement of test setup is shown in **Fig. 4**. The beam was subjected to a four-point bending load. The distance of 200 mm between two loading points was fixed for all specimens. To reduce the horizontal friction between supporting points and beam specimen, the Teflon sheets were placed between supporting points and a specimen. The shear span- effective depth ratio *a/d* for all specimens was 2.8. Two LVDTs were used to monitor the displacement in the mid-span, and another two LVDTs were attached to the supporting points at two sides of the specimen to measure the displacement. As for all specimens, two strain gauges were attached at the center of two tension rebars. For shear reinforcements within shear span, there were strain gauges attached at the region where a diagonal crack was expected to occur. The locations of strain gauges are shown in **Figs. 5**, **6** and **7**. All specimens were applied with a monotonic load up to the failure.

4. THE RESULTS OF BEAM TESTS AND DISCUSSIONS

(1) Load-deflection behaviors and failure modes

The experimental load versus mid-span deflection

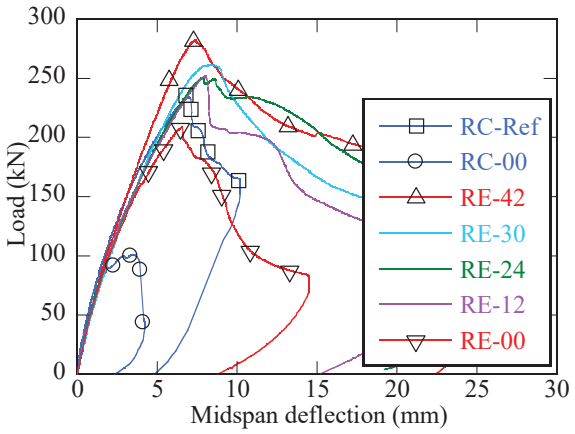

Fig. 8 Load vs. midspan deflection curves for all specimens

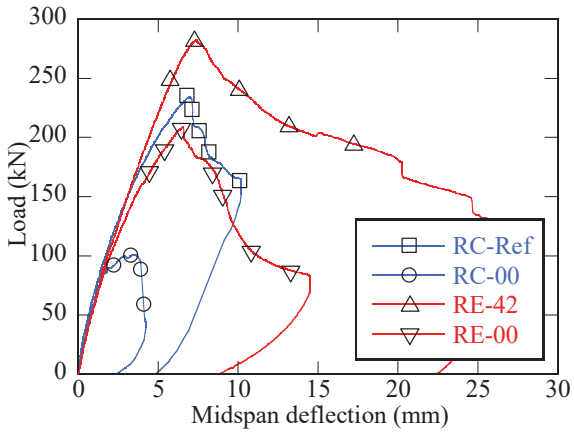

Fig. 9 Load vs. midspan deflection curves forRE-42, 00 and RC-Ref, 00

Table 6 Summary of beam tests

Beam	V_{exp} (kN)	Mid-span deflection (mm)	Compressive strength (MPa)	Tensile strength (MPa)	Tensile yield strength (mm)
RC-Ref	117.03	6.98	29.1	2.53*	–
RC-00	50.27	3.54	34.9	2.88*	–
RE-42	141.09	7.39	30.4	3.67	2.51
RE-30	130.56	8.44	33.1	3.56	2.30
RE-24	125.24	7.89	31.5	3.39	2.38
RE-12	126.05	8.01	35.6	3.68	2.45
RE-00	104.38	6.55	32.8	3.71	2.50

*Tensile strength was obtained by split compression method. The rest were tested by direct tensile tests as described in Chapter 2. V_{exp} is the peak shear force taken by specimens during the tests.

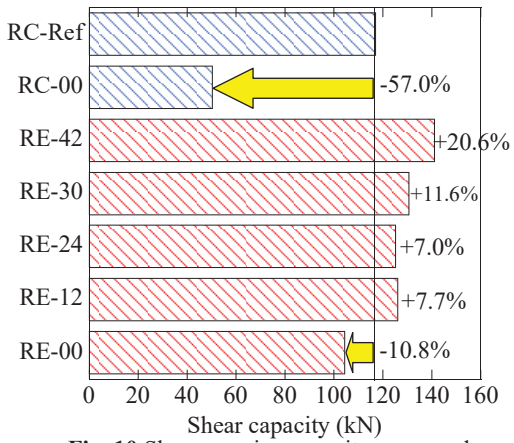

Fig. 10 Shear carrying capacity compared with control beam

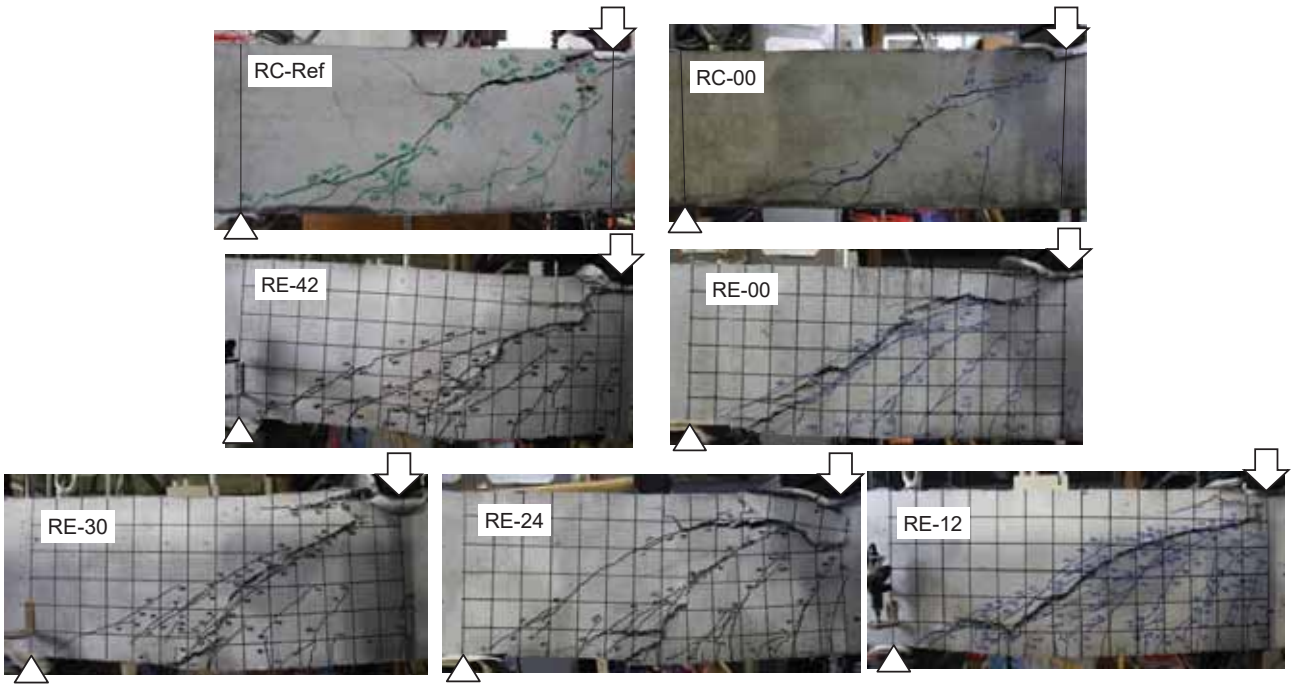

Fig. 11 Failure pattern after loading

curves for all specimens involved in this study are shown in **Figs. 8** and **9**. The mid-span deflection was the average value of displacements obtained by two LVDTs which were set at the center on both sides of a beam. The results of all specimens including material tests are summarized in **Table 6**. The shear carrying capacity by comparing ECC specimens with RC control beam is shown in **Fig. 10**. **Figure 11** shows the failed span at the ultimate stage after loading test. The steel tension rebars for six specimens with shear reinforcements just reached yielding strength at their peak loads but soon decreased as the increase in load as well as development of localization of a critical crack, indicating that all specimens were failed in shear. As for the steel reinforced concrete beam RC-Ref, the first crack appeared in the moment constant region at a load of 54 kN, then inclined shear cracks were induced and propagated with increasing load. The ultimate load capacity of RC-Ref was 234.1 kN. After the peak load, the beam finally failed in crushing and spalling of the concrete in the compression zone of shear span closing to the loading point.

Beam RE-42 had an identical reinforcement layout to that of RC-Ref, except a different matrix, however, the ultimate load capacity was 20.6% higher than that of RC-Ref, achieved 282.2 kN. The first crack load of RE-42 was 86 kN, which was 32 kN greater than that of RC-Ref. Beyond the cracking load, the flexural stiffness decreased slightly but kept almost constant up to the failure. Several diagonal cracks were developed in the shear span, forming as extension of flexural cracks. These shear cracks bent following the compressive stress trajectory with the increase in load. Because of the lower shear span-depth ratio *a/d* (2.8 for all specimens), the beam flexural capacity cannot be fully developed, and then the shear capacity dominates the ultimate load-carrying capacity. The failure of RE-42, similar to that of RC-Ref, was initiated by crushing of ECC at the top compression side of the main shear crack.

RC-00 and RE-00 was a pair of counterpart beam specimens without shear reinforcements compared to the rest of specimens. RE-00 exhibited similar load-displacement behavior to that of RC-00 before the diagonal cracking. Compared with commonly known brittle mode of shear failure such as occurred in RC-00, the shear failure of RE-00 was comparatively gentle and slow. This is due to the bridging effect resulting from PP fibers. At the beginning, vertical flexural cracks firstly appeared at the tensile side of the beam. When the principle tensile stress within a shear span exceeded the cracking strength of ECC, a diagonal crack propagated through the beam web. Instead of appearance of several wide cracks, numerous fine cracks developed in the ECC beams and they spread throughout the shear span. The shear resistance of ECC beam was significantly increased by bridging force carried by fibers. The peak load of RE-00 was 208.76 kN, compared to that of concrete control beam with shear reinforcements (RC-Ref) wherein the load and deflection capacity just decreased by 10.8% and 6%, respectively. However, compared to another counterpart concrete beam without shear reinforcements (RC-00), the load and deflection capacity of RE-00 increased by 107.6% and 85.2%, respectively.

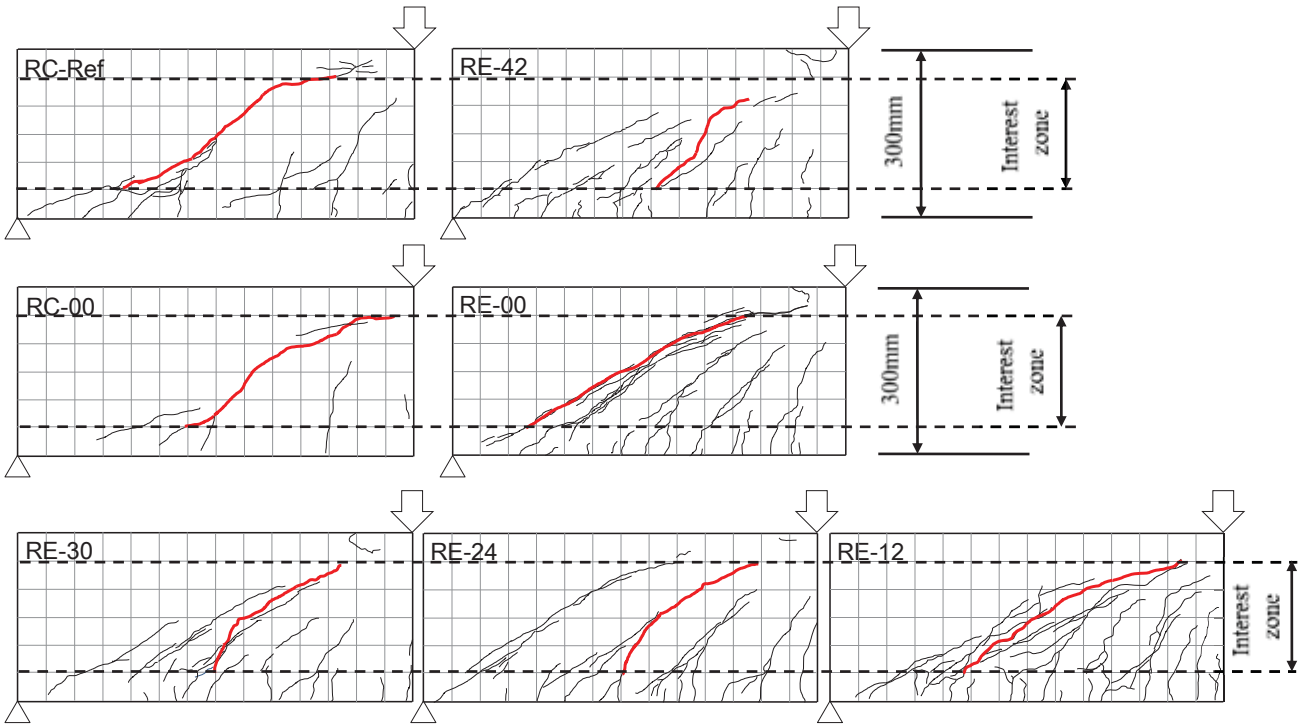

Fig. 12 Cracking behavior at the peak load

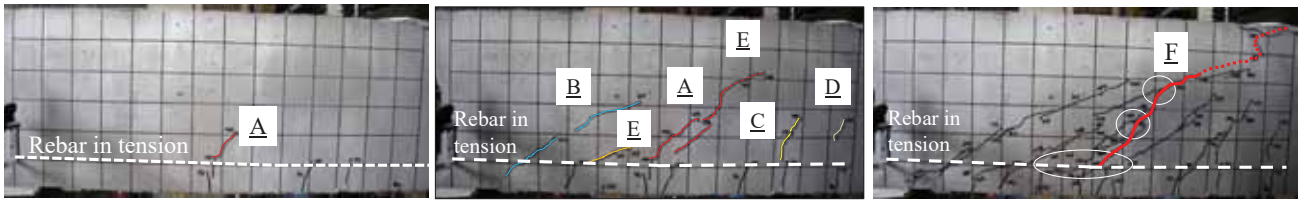

(a) At 110 kN (b) At 170 kN (c) At the peak load

Fig. 13 Development of visible cracks in RE-42

With various shear reinforcement ratios between the level of control beam and zero, RE-30, 24 and 12 were specimens failed in shear similar to that of RE-42. The stiffness of these three beams was found to be slightly higher than that of RE-00 but lower than that of RE-42. The maximum load carried by RE-30, 24 and 12 were 261.1, 250.5 and 252.1 kN, respectively.

(2) Cracking behavior during loading

Figure 12 presents visible cracks of all specimens at the peak load as well as the critical crack developed after the peak load in the interest zone as shown in bold lines with red color. The interest zone for investigation was the zone between longitudinal rebars in tension and compression with height from 50 to 250 mm. The portion above the interest zone adjacent to loading plates was considered as the compression dominating zone due to where the concrete was crushed. In addition, since the tip of diagonal crack in tension stopped propagating at the level of longitudinal tension rebars, and thereby the level of tension rebars was considered as the lower boundary of interest zone.

For RC beams, only one diagonal crack formed at the peak load. Since four to six predominant inclined cracks developed at the web of the beam before the load capacity in each PP-ECC beam, the main diagonal crack was difficult to be identified. After the peak load, as the loading further progressed, these inclined cracks propagated to both supporting and loading plates and the main diagonal crack became more and more distinguishable among these inclined cracks. All five PP-ECC beams exhibited cracking behavior in a similar way. **Figure 13** shows the development of cracking in beam RE-42 in the loading test. Initially, a number of flexural cracks became visible at the edge of beam where subjected to tension. At the load level of 106 kN, first inclined crack A (A in **Fig. 13(a)**) appeared. As the loading up to 170 kN, another three inclined cracks (B, C and D in **Fig. 13(b)**) had been formed. The initially appeared inclined cracks had an angle about from 40° to 50° to the member axis. As the loading progressed, the tip of these cracks began to propagate to supporting and loading plates (E in **Fig. 13(b)**) and some inclined cracks merged with the other existed ones (White line circles in **Fig. 13(c)**). The peak load of a beam was reached before the full development of cracking

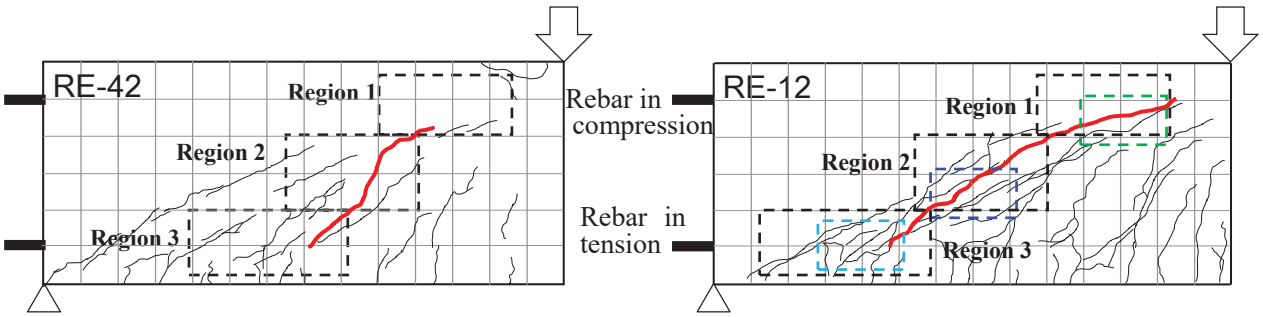

Fig. 14 Regions divided for critical crack

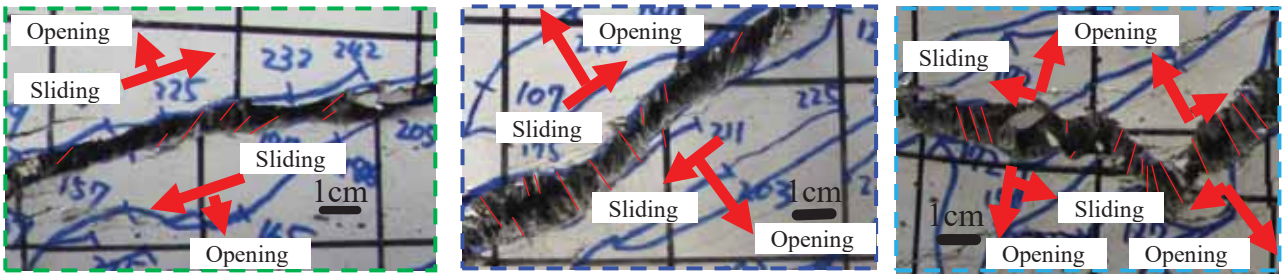

(a) Region 1 (b) Region 2 (c) Region 3

Fig. 15 Critical crack behavior of RE-12 at the ultimate stage

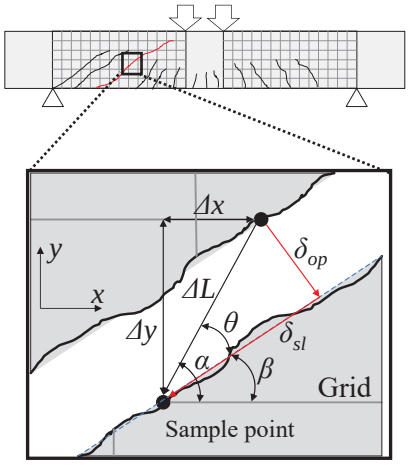

Fig. 16 Displacement of a sample point

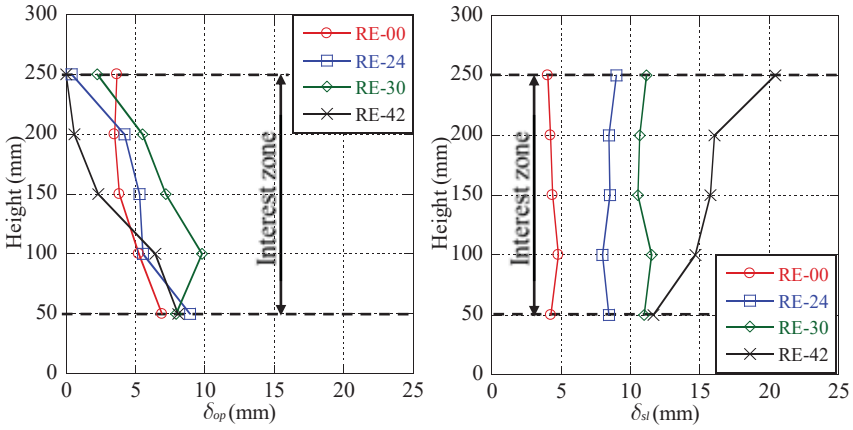

(a) Opening (b) Sliding

Fig. 17 Opening and sliding of the critical crack at 130 kN in post peak stage

propagation. Immediately after the peak load, an inclined crack, as shown in red dot line in **Fig. 13(c)**, propagated into the uncracked compression zone reaching to the loading plates. Meanwhile, the critical crack began to be localized and which propagated to the loading plate was earlier than it came close to the supporting plate. By investigating on the area where the critical crack crossed tension rebars, a number of cracks due to the dowel force developed parallel to tension rebars and propagated to merge with inclined cracks (F area in **Fig. 13(c)**).

According to the above mentioned cracking behavior of RC and PP-ECC beams, the failure mechanism of these two types of beams was considered as follows:

For RC beams, during the propagation of the critical crack, the opening at the critical crack tip simultaneously induced the sliding along the crack surfaces between the crack tip, which in turn develops the significant degree of shear resistance because of the aggregate interlock and rough planes of crack surfaces. The shear resisting factors incorporated shear reinforcements, aggregate interlock along the crack surfaces, dowel action of longitudinal tension rebars and uncracked compression zone. When the critical crack propagated, the maximum shear carrying capacity of RC beam was achieved.

For PP-ECC beams, due to the absence of coarse aggregate, the aggregate interlock effect in PP-ECC beams was significantly weakened. Nevertheless, the fiber bridging contributed substantially to shear transfer resistance. Thus, the shear resisting factors of PP-ECC beams with shear reinforcements during the propagation of shear cracks incorporates shear reinforcements, weakened interlock along the crack surfaces, fiber bridging, dowel action of longitudinal tension rebars and uncracked compression zone. The maximum shear capacity of PP-ECC beams was

achieved when the critical crack propagated into uncracked zone, which led to a sliding failure through the compressive strut.

(3) Investigation on behavior of critical crack

In all five PP-ECC beams, three types of crack paths in the critical crack were observed. Therefore, the critical crack was divided into three regions, namely, Region 1, 2 and 3. For beam RE-42 and RE-12, three regions were divided as shown in **Fig. 14**. In Region 1, the inclination of crack surface was comparatively flat. The crack surface in this region was smoother than that in Region 3. Fewer ruptured PP fibers extended out of crack surface, as shown in **Fig. 15(a)**, could be observed compared to that of Region 2. Some remaining fibers extended out of crack surface oriented to the direction of relative displacement of two surfaces occurred as shown in **Fig. 15(a)**. In Region 2, the angle of crack to the beam axis was about 45°. Compared with Region 1, fibers out of crack surface became more and they tended to be perpendicular to crack surface, as shown in **Fig. 15(b)**. In Region 3, the critical crack formed at the level of rebar in tension, and the surface of crack was jagged and a number of fine cracks occurred close to the critical crack. Quantity of visible fibers in this region was the most among these three regions. Most fibers were oriented to the direction which perpendicular to crack surface, as shown in **Fig. 15(c)**. Since the tension rebars crossed the critical crack, the jagged crack was considered to be formed because of the dowel action of longitudinal bars, which tended to separate the cover of ECC off.

It was considered that the damage induced by ruptured PP fibers resulting from sliding on the critical crack surfaces for each PP-ECC beam at the peak load was different. Therefore, more significant sliding on the critical crack surfaces could be observed at the post peak stage in the PP-ECC beam due to more ruptured fibers at the peak load. Therefore, to further investigate the damage induced by sliding of the critical crack surfaces in the post peak stage, the grid with unit square size of 50mm×50mm was marked on the side surface of beam specimens prior to the loading tests. Those points at where the critical crack crossed horizontal lines of the grid were selected for sample points. By measuring their horizontal displacement (Δx) and vertical displacement (Δy) as shown in **Fig. 16**, the resultant displacement (ΔL) of a sample point and its angle (α) to horizontal axis can be calculated by Eq. (1) and (2), respectively.

$$\Delta L = \sqrt{\Delta x^2 + \Delta y^2} \tag{1}$$

$$\alpha = \arctan\frac{\Delta y}{\Delta x} \tag{2}$$

The resultant displacement consists of two displacements resulting from the crack opening (δ_{op}) which is perpendicular to the crack surface and the crack sliding (δ_{sl}) which is along the crack surface. According to **Fig. 16**, the opening and sliding of the critical crack could be calculated by Eq. (3) and (4), respectively.

$$\delta_{op} = \Delta L \cdot \sin\theta \tag{3}$$

$$\delta_{sl} = \Delta L \cdot \cos\theta \tag{4}$$

where, δ_{op} and δ_{sl} are opening and sliding of the critical crack, θ is the angle of resultant displacement to the crack surface. θ can be obtained by Eq. (5):

$$\theta = \alpha - \beta \tag{5}$$

where, β is the average angle of the critical surface to horizontal axis in one grid.

The calculated opening and sliding of the critical cracks along the height of a beam in the interest zone for four PP-ECC beams (RE-42, RE-30, RE-24 and RE-00) at the load level of 130 kN in the post peak stage were presented in **Fig. 17**. **Figure 17(a)** shows that the opening of the critical crack along the beam height in the interest zone, indicating the opening decreases as the increase in the beam height for four PP-ECC beams investigated. However, the relationship between the opening and shear reinforcement ratio was difficult to be observed. **Figure 17(b)** shows the sliding of the critical crack along the beam height. It indicates more

Table 7 Angle of critical crack in interest zone

Beams	RE-42	RE-30	RE-24	RE-12	RE-00
Angle (°)	43.9	40.3	39.3	27.3	26.5

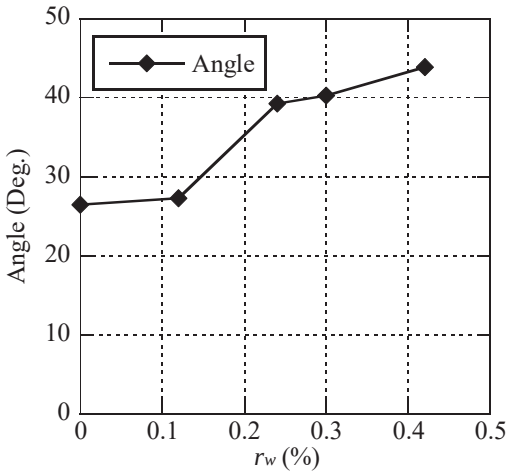

Fig. 18 Angle of critical crack for PP-ECC beams

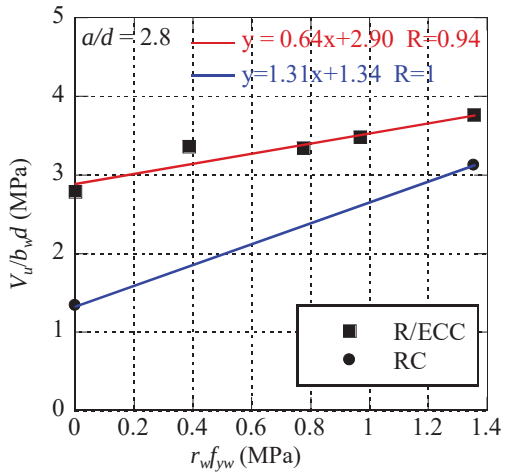

Fig. 19 Shear stress versus shear reinforcements

Table 8 Shear resisting proportion of V_{ECC} or V_{con} and V_s

Beam	V_{exp} (kN)	V_{ECC_exp} or V_{c_exp} (kN)	V_{s_exp} (kN)	V_{ECC_exp} or V_{c_exp} (%)	V_{s_exp} (%)
RC-Ref	117.0	45.1	71.9	39%	61%
RC-00	50.3	50.3	0.0	100%	0%
RE-42	141.1	59.3	81.8	42%	58%
RE-30	130.6	69.6	61.0	53%	47%
RE-24	125.2	84.3	40.9	67%	33%
RE-12	126.1	105.6	20.5	84%	16%
RE-00	104.4	104.4	0.0	100%	0%

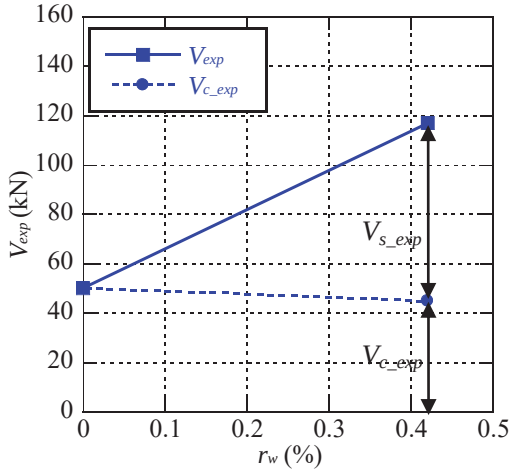

Fig. 20 Experimental shear proportion of two RC beams

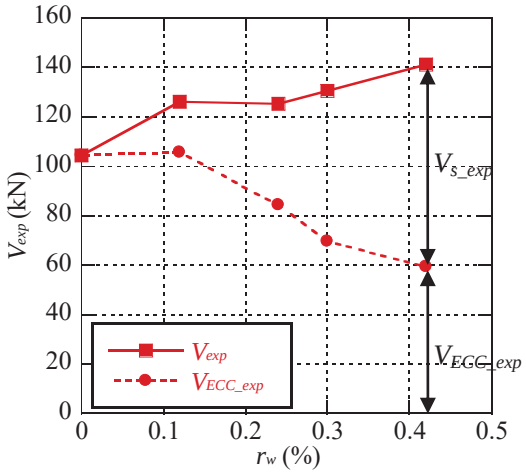

Fig. 21 Experimental shear proportion of five PP-ECC beams

significant sliding displacement on the critical crack surfaces in PP-ECC beams with larger shear reinforcement ratio, which further reveals that the damage to fiber bridging induced by sliding on the critical crack surfaces in PP-ECC beam with higher shear reinforcement ratio at the peak load is more significant.

(4) Shear cracking angle of PP-ECC beams

As shown in **Fig. 12**, the angles of the critical cracks in the interest zone at the peak load for five PP-ECC beams were measured. The angle was determined as the beam axis to the line which linked points crossed by the critical crack with upper and lower boundary of the interest zone. The angle of critical crack to the beam axis for five PP-ECC specimens were listed in **Table 7**. The relationship between the angle of critical crack and shear reinforcement ratio, as shown in **Fig. 18**, shows that the critical crack of PP-ECC beams with more shear reinforcements become more steeper, which implies that the development of critical crack was suppressed in PP-ECC beams with increasing shear reinforcement ratio r_w. The steeper critical cracks results in shorter diagonal crack length and thereby reduced the shear carried by PP fibers in ECC.

(5) Effect of shear reinforcement ratio

As confirmed by previous extensive experimental studies[12], for RC beams with shear reinforcements governed by shear failure, the shear capacity will increase significantly as increase of shear reinforcement ratio. **Figure 19** shows the relationship between shear capacity of beams and quantity of shear reinforcements in this study, in which, V_u is the maximum shear applied to specimens, r_w is shear reinforcement ratio and f_{yw} is the yield strength of shear reinforcement. The shear capacity of PP-ECC beams did not increase significantly as that of RC beams with the increase in shear reinforcement ratio.

Although the shear capacity of RC beams increases with the increase in shear reinforcement ratio, it should be noted that the shear taken by concrete can be assumed to be almost constant with varying of shear reinforcement ratio, which has been experimentally demonstrated. In JSCE code, the shear taken by concrete (V_c) was defined as Eq. (6):

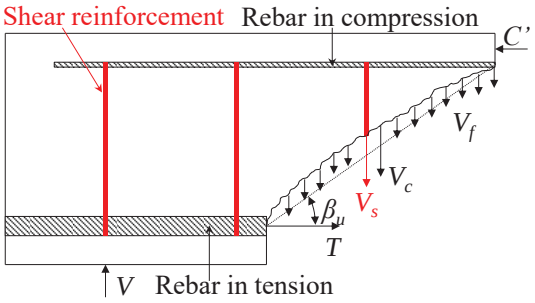

Fig. 22 Free body diagram of PP-ECC beam

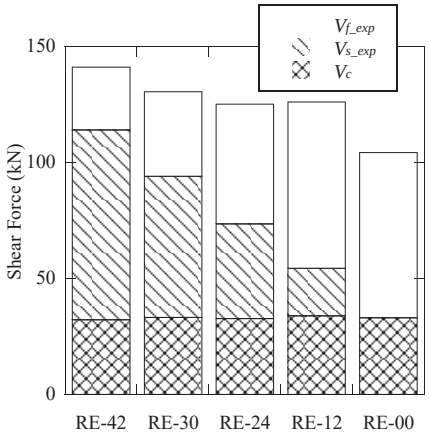

Fig. 23 Shear forces of PP-ECC beam

$$V_c = 0.20\sqrt[3]{f'_c}\cdot\sqrt[4]{1/d}\cdot\sqrt[3]{100\,p_w}\cdot b_w\cdot d \qquad (6)$$

where, V_c is the shear force carried by concrete (N), f'_c is compressive strength of concrete (MPa), d is effective depth (m), p_w is longitudinal reinforcement ratio and b_w is the web thickness (mm). The experimental shear carried by shear reinforcements (V_{s_exp}) can be obtained from the strain of shear reinforcements which the critical diagonal crack crossed. The strain of shear reinforcements was captured by strain gauges attached on the shear reinforcements during the tests. Thus, the shear carried by shear reinforcements (V_{s_exp}) can be formulated by Eqs. (7) and (8).

$$V_{s\_exp} = \sum_{i=1}^{n_s} A_w \sigma_{si} \qquad (7)$$

$$\sigma_{si} = \begin{cases} E_s\varepsilon_{si} \left(\varepsilon_{si} < \varepsilon_y\right) \\ f_{wy} \left(\varepsilon_{si} \geq \varepsilon_y\right) \end{cases} \qquad (8)$$

where, n_s is the number of shear reinforcements crossing the critical crack, σ_{si} is the stress of shear reinforcement crossing a critical crack at the peak load, A_w is cross sectional area of a pair of shear reinforcements within s (mm^2), E_s is the elastic modulus of shear reinforcement, ε_s is the stirrup strain recorded in the tests, ε_y is the yielding strain of shear reinforcements listed in **Table 3**. The total

Table 9 Experimental and calculation results of shear forces

Beam	V_{exp} (kN)	V_c (kN)	V_{s_exp} (kN)	V_{f_exp} (kN)	V_{f_cal} (kN)	$v=\frac{V_{f\_exp}}{V_{f\_cal}}$
RE-42	141.1	32.3	81.8	27.0	85.1	0.32
RE-30	130.6	33.2	61.0	36.4	88.4	0.41
RE-24	125.2	32.7	40.9	51.6	95.0	0.54
RE-12	126.1	34.0	20.5	71.6	154.7	0.46
RE-00	104.4	33.1	0.0	71.3	163.3	0.44

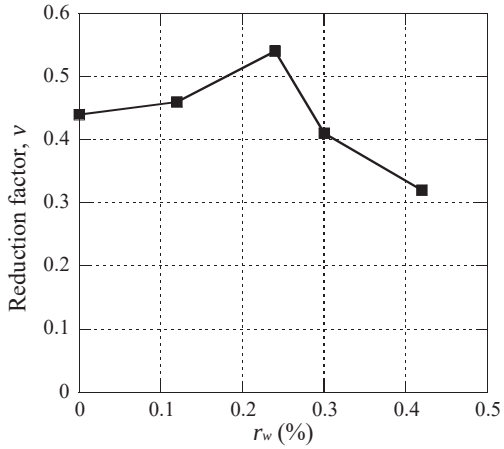

Fig. 24 Reduction factor for the shear carried by fibers

shear carried by PP-ECC and RC beams can be formulated by Eqs. (9) and (10), respectively.

$$V_{exp} = V_{ECC\_exp} + V_{s\_exp} \qquad (9)$$

$$V_{exp} = V_{c\_exp} + V_{s\_exp} \qquad (10)$$

where, V_{ECC_exp} is the experimental shear carried by ECC for PP-ECC beams, V_{c_exp} is the experimental shear carried by concrete for RC beams. From Eqs. (7) to (10), V_{ECC_exp} and V_{c_exp} can be calculated by Eqs. (11) and (12), respectively.

$$V_{ECC\_exp} = V_{exp} - V_{s\_exp} \qquad (11)$$

$$V_{c\_exp} = V_{exp} - V_{s\_exp} \qquad (12)$$

The experimental value of shear taken by shear reinforcements and matrix (ECC or concrete) is listed in **Table 8**. The experimental shear resisting components versus shear reinforcement ratio (r_w) for RC and PP-ECC beams were plotted as shown in **Figs. 20** and **21**, respectively. For two RC beams, as shown in **Fig. 20**, the shear taken by concrete was almost constant even as the variation of shear reinforcement ratio, whereas the shear taken by shear reinforcements (V_{s_exp}) increased proportional to the shear reinforcement ratio. For five PP-ECC beams, as shown in **Fig. 21**, the tendency of shear carried by PP-ECC was decreasing as the increase in shear reinforcement ratio while the shear carried by shear reinforcement increased as the increase in shear re-

inforcement ratio. Since the increase of shear carried by shear reinforcements was more significant than the decrease of shear carried by PP-ECC, as a result that the reinforcing effect of shear reinforcements in PP-ECC beams is not significant as that of RC beams.

5. EVALUATION OF REDUCTION ON SHEAR CARRIED BY PP-ECC

So far, several researchers[8),9)] have attempted to develop some models to evaluate the shear strength of PP-ECC structural members. The currently available simplified models are the truss-and-arch model based on recommendation of AIJ for RC structural members[13)], and modified truss model recommended by JSCE, which incorporated an equation accounting for the shear carried by fibers (V_f). Both models mentioned above incorporated the shear carried by fibers independently by employing an equation. In this study, the shear carried by PP-ECC structural members followed Recommendations for Design and Construction of HPFRCC by JSCE[7)]. JSCE recommendations evaluate the shear strength of R/ECC beams by summing up the shear resisting factors, as shown in **Fig. 22** and expressed by Eq. (12).

$$V = V_c + V_s + V_f \tag{12}$$

where, V represents calculated total shear capacity of ECC structural member, V_c, V_s and V_f represent shear carried by members without shear reinforcements excluding the fiber effects, shear reinforcements and fibers, respectively. V_c is similar to the equation that is defined in JSCE code for RC structural members, but a reduction factor of 0.7 is incorporated because ECC allows cracks in service, which is expressed by Eq. (13).

$$V_c = 0.7 \times 0.20 \cdot \sqrt[3]{f'_{ECC}} \cdot \sqrt[4]{1/d} \cdot \sqrt[3]{100 p_w} \cdot b_w \cdot d \tag{13}$$

where, V_c is the shear carried by members without shear reinforcements excluding the fiber effects, f'_{ECC} is compressive strength of ECC (MPa), d is effective depth (m), p_w is longitudinal reinforcement ratio and b_w is the web thickness (mm).

The experimental and calculation values of shear carried by fibers can be obtained by Eqs. (14) and (15).

$$V_{f\_exp} = V_{exp} - V_c - V_{s\_exp} \tag{14}$$

$$V_{f\_cal} = \left(f_{ty} / \tan \beta_u \right) \cdot b_w \cdot z \tag{15}$$

where, f_{ty} is the yield tensile strength of ECC determined based on the stress-strain relationship immediately after the first cracking based on the testing method described in **Chapter 2** (MPa), β_u is the angle of diagonal crack surface to the member axis, taking the value listed in **Table 7**.

Table 9 lists experimental and calculation results of shear forces. The values of V_c, V_{s_exp}, V_{f_exp} and V_{f_cal} were calculated from Eqs. (13), (8), (14) and (15), respectively. As shown in **Fig. 23**, the experimental value of shear carried by fibers decreased as the increase in shear reinforcement ratio resulted from the rupture of PP fibers due to more significant sliding along the critical crack in PP-ECC beams with more shear reinforcement. For the shear carried by fibers, a reduction factor, which was defined as the ratio of experimental value to calculation value as expressed by Eq. (16) and listed in **Table 9**, was used to account for the reduced shear due to sliding.

$$v = V_{f\_exp} / V_{f\_cal} \tag{16}$$

As shown in **Fig. 24**, the value of a reduction factor ranges from 0.32 to 0.54 and its trend is that the value decreases as the increase in shear reinforcement ratio, which indicates that the shear carried by fibers in ECC beams with dense shear reinforcements is smaller than that with less shear reinforcements. Therefore, it was concluded that the the reduced shear carried by fibers due to the increase in shear reinforcement ratio was not considered in JSCE code, which may result in overestimation on the shear capacity of ECC structural members.

6. CONCLUSIONS

This paper describes the shear behavior of PP-ECC beam specimens with various shear reinforcement ratios by experimental investigation. Totally seven beams, such as two normal steel reinforced concrete and five steel reinforced PP-ECC beams, were tested under static monotonic loading condition. The following conclusions could be deduced.

1) Since the absence of coarse aggregate in PP-ECC, attributing to the fiber bridging effect in PP-ECC, the shear carrying capacity of the beam with shear reinforcements and without shear reinforcements increased 20.6% and 107.6%, respectively by replacing concrete with

PP-ECC. The shear carrying capacity can be increased by replacing cement matrix from concrete to PP-ECC, especially in case of lower shear reinforcement ratio.

2) The damage to fiber bridging effect induced by sliding on the critical crack surfaces in PP-ECC beam with higher shear reinforcement ratio at the peak load is more significant compared to the case with lower shear reinforcement ratio, which becomes one of factors resulting in shear carried by ECC in PP-ECC beams decreases as the increase in shear reinforcement ratio.
3) The angle of critical crack to the beam axis in PP-ECC beam decreases as the increase in shear reinforcement ratio, which simultaneously triggers in reduction on the shear carried by fibers along the critical crack, becoming another factor resulting in the reduction on shear carried by PP-ECC as the increase in shear reinforcement ratio.
4) Different from the case of shear resisting proportion in RC beams, in which the shear carried by concrete is almost constant even with varying shear reinforcement ratios and the shear carried by shear reinforcement is proportional to shear reinforcement ratio, the shear carried by ECC in PP-ECC beams decreases as the increase in shear reinforcement ratio. This decrease of shear carried by fibers results from combined action between the reduction on shear carried by fibers along the critical crack and increased damage to fiber bridging induced by sliding along the critical crack surfaces.
5) The current JSCE code does not take the factors that the reduction on shear carried by fibers in ECC due to sliding as the increase in shear reinforcement ratio into consideration which may result in overeastimation on shear capacity of PP-ECC structural members.

ACKNOWLEDGMENT: This research was supported by Young Researcher Fund from the Center for Urban Earthquake Engineering (CUEE) in Tokyo Institute of Technology.

REFERENCES

1) Li, V. : Engineered Cementitious Composites (ECC) – Tailored Composites through Micromechanical Modeling, Fiber Reinforced Concrete : Present and the Future, eds. N. Banthia, and A. Mufti, Canadian Society of Civil Engineers, pp. 64-97, 1998.
2) Maalej, M. and Li, V. : Flexural/Tensile-strength Ratio in Engineered Cementitious Composites, *Journal of Materials in Civil Engineering*, ASCE, Vol. 6, No. 4, pp. 513-528, 1994.
3) Brown, R., Shukla, A. and Natarajan, K. R. :Fiber reinforcement of concrete structures, *University of Rhode Island Transportation Center (URITC) Project No. 536101*, 2002.
4) Hirata, T., Kawanishi, T., Okano, M. and Watanabe, S. : Study on Material Properties and Structural Performance of High-Performance Cement Composites Using Polypropylene Fiber, *Proc. of Japan Concrete Institute*, Vol. 31, No. 1, pp. 289-294, 2009. (Japanese)
5) Li, V. and Fischer, G. : Effect of Matrix Ductility on Deformation Behavior of Steel Reinforced ECC Flexural Members under Reversed Cyclic Loading Conditions, *ACI Structural Journal*, Vol. 99, No. 6, pp. 781-790, 2002.
6) Shimizu, K., Kanakubo, T., Kanda, T. and Nagai, S. : Shear Behavior of Steel Reinforced PVA-ECC Beams, *13th World Conference on Earthquake Engineering*, Canada, 2004.
7) JSCE : *Recommendations for Design and Construction of High Performance Fiber Reinforced Cement Composites with Multiple Fine Cracks (HPFRCC)*, Japan Society of Civil Engineers, 2008.
8) Kanakubo, T., Shimizu, K., Kanda, T. and Nagai, S. : Evaluation of Bending and Shear Capacity of HPFRCC Members Toward the Structural Application, *Proc. of Hokkaido University COE Workshop on High Performance Fiber Reinforced Composites for Sustainable Infrastructure System- Material modeling, Structural Design and Application*, Sapporo, Japan, 2007.
9) Suryanto, B., Nagai, K. and Maekawa, K. : Modeling and Analysis of Shear-critical ECC Members with Anisotropic Stress and Strain Fields, *Journal of Advanced Concrete Technology*, Vol. 8, No. 2, pp. 239-258, 2010.
10) Kabele, P., and Kanakubo, T. : Experiential and Numerical Investigation of Shear Behavior of PVA-ECC in Structural Elements, *Proc. of 5th International RILEM Workshop on High Performance Fiber Reinforced Cement Composites (HPFRCC5)*, Reinhardt and Naaman, eds., pp. 137-146, 2007.
11) Parra-Montesinos, J. G., Peterfreund, W. S., and Chao, S. : Highly Damage-Tolerant Beam-Column Joints Through Use of High-Performance Fiber-Reinforced Cement Composites, *ACI Structural Journal*, May-June 2005.
12) Leonhardt, F. : Reducing the Shear Reinforcement in Reinforced Concrete Beams and Slabs, *Magazine of Concrete Research*, Vol. 17, No. 53, pp. 187-198, 1965.
13) Architectural Institute of Japan : *Design Guidelines for Earthquake Resistant Reinforced Concrete Buildings Based on Ultimate Strength Concept*, pp. 106-116, 1990.